INTERACTION VERSUS RADIO SOURCE GENERATION: THE PROPERTIES OF RADIO JET PARENT GALAXIES

L. COLINA[1,2]
Space Telescope Science Institute

AND

I. PÉREZ-FOURNON[1]
Instituto de Astrofísica de Canarias, Tenerife, Spain
Received 1989 April 3; accepted 1989 July 13

ABSTRACT

A sample of 47 galaxies with radio jets from the Bridle and Perley list with $z \leq 0.15$ and $\delta \geq -15°$ has been observed with CCD two-dimensional imaging (Colina and Pérez-Fournon).

As much as 50% of the sample presents morphological peculiarities like isophote twists, nonconcentric isophotes, filaments, or a large companion galaxy present. This fraction agrees with previous values obtained for high-luminosity radio galaxies (Hutchings; Heckman *et al.*). Considering projection effects, at least 35% of the radio jet galaxies are undergoing physical interaction with another elliptical galaxy.

Of the present sample, 45% of the galaxies (21) are classified as dumbbell (six) or have a companion galaxy, mean relative size 0.37 that of the radio source, at projected distances shorter than 20 kpc (15). These galaxies, the multicomponent sample, present a very homogeneous set of radio properties: 67% have $22.0 \leq \log P^{\rm core}_{5\,\rm GHz} \leq 23.0$ WHz^{-1}; 67% have $24.0 \leq \log P^{\rm total}_{1.4\,\rm GHz} \leq 25.0$ WHz^{-1}; 67% have $10 \leq d_{\rm jet} \leq 40$ kpc; 71% have $0.00 \leq P^{\rm core}_5/P^{\rm total}_{1.4} \leq 0.03$. A parameterization of the companion galaxies within 20 kpc of the radio galaxy nucleus is done in terms of number, size, and gravitational potential.

The rest of the sample, consisting of galaxies with no companions at distances shorter than 20 kpc, isolated sample, appears as more heterogeneous, with a large fraction presenting characteristics of gas-rich galaxies.

We conclude that multicomponent galaxies are associated with physical interaction between elliptical galaxies, e.g., 3C 465, 3C 278, or B2 0206+35. On the other hand, our isolated galaxies are most likely associated with gas-rich galaxies, e.g., 3C 120, with interactions/merging involving gas-rich galaxies, e.g., 3C 305, or with elliptical galaxies, some of them showing a very compact core, e.g., 3C 303 or 3C 371.

The differences in the radio properties are explained as a consequence of a different optical parent galaxy population and interaction effects. Galaxies with gas produce more powerful radio sources than those without. Also, interactions seem to control, at least when ellipticals are involved, the process of energy generation, producing a very well defined class of radio sources.

Subject headings: galaxies: interactions — galaxies: jets — galaxies: structure — radio sources: galaxies

I. INTRODUCTION

It is well known that active galaxies in general and radio galaxies in particular inhabit regions of higher local galaxy density than normal field galaxies (Kennicutt and Keel 1984; Dahari 1984; Heckman *et al.* 1984, 1985; Fricke and Kollatschny 1986).

Studies of the surrounding intergalactic medium of radio galaxies at 1 Mpc size scale (Stoke 1979) indicate an anticorrelation between the size of the radio emission regions and the galaxy density of the surrounding intergalactic medium. Also Shaver and collaborators (1982) showed that, among radio galaxies, a more distorted radio morphology is observed as the distance to a companion galaxy decreases. They concluded that both C and S distortions of the radio structure are associated with the presence of other nearby (distances within a few hundred kpc) galaxies.

Stocke (1978) showed that close pairs are radio sources at more than twice the number of more widely spaced pairs. Very

recently, Vettolani and Gregorini (1988) also stressed this fact. They concluded that for elliptical or lenticular galaxies, the membership to a group or a cluster does not seem to trigger the mechanism of radio emission; on the contrary, they found a correlation between the presence of a radio source and close companions (separation less than 100 kpc).

Orbital motions (Wirth, Smarr, and Gallagher 1982) or precessional effects (Begelman, Blandford, and Rees 1980) have been invoked to explain the C and S morphologies. Also, recent studies of high-luminosity radio galaxies (log $P_{408\,\rm MHz} \geq 25.5$ WHz^{-1}; Heckman *et al.* 1986) show that 25%–30% of the galaxies have strongly peculiar optical morphology. This is interpreted as an indication of interaction/merging processes between galaxies.

In view of all the previous evidences, considering that nonthermal radio activity originates at the core of the galaxies and propagates into the interstellar/intergalactic medium through the jets, it is of fundamental importance to study the nature of the parent radio jet galaxy as well as the effect of very close nearby companions in the origin and maintenance of this activity.

We have started a large observational program to cover a representative sample of radio galaxies containing radio jets in

order to study the optical properties of the parent galaxy as well as to detect optical emission associated with the radio structures.

A complete catalog of the galaxies under the present study can be found in Colina and Pérez-Fournon (1989, hereafter Paper I), while analysis of individual galaxies have been published elsewhere (M87: Pérez-Fournon et al. 1988; 3C 433: Colina and Pérez-Fournon 1990). In this paper, a statistical study of the properties of the sample presented in Paper I is discussed in terms of differences in parent galaxies and inter-action effects. Since most of the radio jet galaxies are low-luminosity radio sources (see § IIa), this study is complementary to these based in a sample of high-luminosity radio galaxies (Baum et al. 1988; Baum and Heckman 1989a, b). Throughout this paper $H_0 = 75$ km s^{-1} Mpc^{-1} will be used.

II. THE DATA

a) The Sample

The sample object of this study was selected from the Bridle and Perley (1984) list of galaxies containing well-defined radio jets considering $0.01 \leq z \leq 0.15$ and $\delta \geq -15°$. This sample, which is optically unbiased, cannot be considered as complete in any sense, although the presence of the same radio jet emission morphology can be seen as evidence of some physical mechanism at work. Considering the radio luminosity at 1.4 GHz, the sample is of low to intermediate luminosity, median $\log P^{total}_{1.4} = 24.83$ WHz^{-1}, with all but six galaxies with $P^{tot}_{1.4} \leq 10^{25}h_0^{-2}$ WHz^{-1} ($h_0 = H_0/100$). If, on the other hand, one con-siders the radio structure, all the galaxies but 10 show two-sided jet morphology according to Bridle criteria of sideness (Bridle 1984). In conclusion, the sample can be considered as formed by low-luminosity Fanaroff-Riley type I galaxies. Details on the optical morphological characteristics of these objects have been published in a separate paper (Paper I).

b) Observations and Data Reduction

All the observations were done at the Calar Alto Observa-tory of the Max-Planck Society using an RCA CCD camera with a field of view of $112'' \times 180''$. This instrument was attached to the 2.2 m telescope and the r-filter of the Gunn-Thuan system was used (Thuan and Gunn 1976). The data reduction, consisting of bias subtraction, flat-field correction, and background subtraction, was done in the standard way. For more details both on the observations and data reduction see Paper I.

c) Data Analysis

Since the present study investigates the relations between the radio properties of galaxies with radio jets and their optical characteristics, parameters, or magnitudes defining the radio galaxy and the parent optical galaxy are needed.

The Bridle and Perley (1984) list is considered as the unique reference with an homogeneous set of radio data. Therefore, the total radio luminosity at 1.4 GHz ($\log P^{total}_{1.4}$), the core radio luminosity at 5 GHz ($\log P^{core}_5$), the linear size of the jet (d_{jet}; the larger one is considered in case of two-sided jets) and the core to total radio luminosity ratio ($P^{core}_5/P^{total}_{1.4}$) are considered as the fundamental parameters to define the radio galaxy (see Table 1). In order to have all absolute luminosities scaled to the same Hubble constant, both $\log P^{total}_{1.4}$ and $\log P^{core}_5$ have been rescaled to $H_0 = 75$ km s^{-1} Mpc^{-1} from the original values of Bridle and Perley (1984) where they used $H_0 = 100$ km s^{-1} Mpc^{-1}. This rescaling has also been applied to the

TABLE 1
RADIO PROPERTIES OF THE SAMPLE GALAXIES

Name	$\log P^{total}_{1.4}$ WHz^{-1}	$\log P^{core}_5$ WHz^{-1}	$P^{core}_5/P^{total}_{1.4}$	d(jet) kpc
NGC 315	24.33	23.49	0.1445	330.0
NGC 326	24.86	22.54	0.0048	33.3
3C 31	24.46	22.70	0.0174	18.7
NGC 541[a]	24.02	21.97	0.0089	18.0
NGC 708	22.87	21.56	0.0490	6.0
0206+35	24.77	23.40	0.0427	24.0
3C 66B	24.94	22.84	0.0079	60.0
NGC 1044	24.05	22.79	0.0214	57.3
3C 75	24.86	22.65	0.0062	40.0
4C 1317B	24.32	22.55	0.0748	20.0
3C 78	25.08	24.02	0.0871	0.8
NGC 1265	25.01	22.40	0.0025	24.0
3C 84	24.91	25.12	1.6218	6.7
0326+39	24.31	22.95	0.0437	54.7
3C 111	25.84	24.72	0.0759	104.0
3C 120	25.01	25.18	1.4791	110.7
3C 129	24.83	22.44	0.0041	11.7
0658+32	25.07	24.23	0.1445	73.3
4C 3516A	24.53	22.08	0.0035	22.7
4C 5316	25.08	23.21	0.0135	17.3
0908+37	25.14	23.75	0.0407	30.7
NGC 4789	23.80	21.41	0.0041	8.9
3C 278	24.48	22.38	0.0079	18.7
NGC 4869	23.14	21.33	0.0155	3.5
4C 2947	25.10	23.50	0.0251	146.7
NGC 5127	24.10	22.02	0.0083	73.3
NGC 5490	23.93	22.25	0.0209	7.3
3C 296	24.68	22.92	0.0174	66.7
3C 303	26.00	24.78	0.0603	34.7
3C 305	24.98	22.82	0.0069	1.2
1450+28	24.81	22.81	0.0100	18.7
A2172	24.45	23.45	0.1000	18.7
4C 5337	25.18	23.46	0.0191	53.3
3C 371	25.09	24.85	0.5754	2.7
3C 388	25.98	24.01	0.0107	24.0
4C 4751	25.11	23.44	0.0214	353.3
3C 402N	24.56	22.33	0.0059	8.3
3C 405	27.98	24.37	0.0002	62.7
NGC 7052	22.97	22.37	0.2512	34.7
3C 433	26.40	23.01	0.0004	40.0
3C 445	25.55	23.76	0.0162	280.0
3C 449	24.28	22.32	0.0110	25.3
2236+35	23.65	22.13	0.0277	10.3
OZ 127	23.95	22.66	0.0513	21.3
NGC 7626	23.42	21.56	0.0138	8.5
3C 465	25.10	23.62	0.0331	32.0
4C 4763	24.88	22.74	0.0072	49.3

[a] Values obtained from van Breugel et al. 1985. Core luminosity obtained using $\alpha = 0$ as in Bridle and Perley 1984.

linear size of the jet. Other properties, like magnetic field con-figuration, bending angles, or radio spectral index, appear more scarcely in the literature or depend on spatial resolution. Therefore, these have not been included in this study.

To characterize the optical parent galaxy, no parametriza-tion based in absolute photometry, such as the magnitude and surface brightness within a radius of 19 kpc centered on the radio galaxy (Lilly and Prestage 1987), has been done. The reason for that is that in our sample, 45% of the galaxies appear with companions of different sizes at distances shorter than 20 kpc, i.e., well inside the main body of the radio galaxy. Then, too, it is difficult to obtain reliable parameters without a detailed decomposition of the common isophote structure. Therefore the main parameters for classifying the parent galaxy are related to morphological features at an estimated surface brightness brighter than 23–24 mag arcsec^{-2}. Among

these, we have considered isophote twists, presence of nuclear dust lanes (using not calibrated g-r maps), and existence of other peculiar morphological features such as filaments, isophotes, off-centering, or asymmetric light distributions (see Table 2 for details).

The absolute visual magnitude (obtained from the m_v and redshift values presented in Paper I considering galactic extinction corrections, $H_0 = 75$ km s^{-1} Mpc^{-1} and $q_0 = 0$), together with the 60 μm luminosity and the 60 μm/100 μm luminosities ratio from the Golombek, Miley, and Neugebauer (1988) compilation are considered as parameters characterizing the optical properties of the parent galaxy (see Table 2). Also the presence of emission lines in the spectra has been considered.

Almost half of the present sample shows a dumbbell morphology, i.e., two equal size galaxies sharing a common envelope (0255+05 or 1252−12 can be considered as

archetypes), or a smaller companion, i.e., any extended object with a size at least 0.1 times that of the radio galaxy, at distances shorter than 20 kpc (0206+35, 0326+39, or 2335+26 can be considered as archetypes). Then, taking also into consideration the CCD size limitations, a parametrization of the radio galaxy environment within a radius of 20 kpc for all galaxies with a redshift $0.01 \leq z \leq 0.15$ has been done.

This parametrization consist in a set of parameters related to the number, size, distance, and gravitational potential of the companion galaxies inside a certain radius:

$$P_n = N, \quad P_s = \sum_i^n \frac{D_i}{D_R}, \quad P_d = \sum_i^n \frac{100}{d_{ir}},$$

$$P_g = \sum_i^n \left(\frac{D_i}{D_R}\right)^{1.5}\left(\frac{100}{d_{ir}}\right),$$

TABLE 2

OPTICAL PROPERTIES OF THE SAMPLE GALAXIES

Name	M_v	Morphology[a]	Spectra	$\log \dfrac{L(60\ \mu\text{m})}{L_\odot}$	$R[\ F(60\ \mu\text{m})/F(100\ \mu\text{m})]$
NGC 315	−21.75	NP	A	9.41	0.80
NGC 326	−23.63	db, TWI	A	...	...
3C 31	−22.07	P, D, CE	A	9.48	0.26
NGC 541	−21.32	TWI	A	...	...
NGC 708	−19.64	P, TWI, D	E	<9.22	<0.30
0206+35	−23.11	P, TWI, D, CE	A	<9.66	<0.41
3C 66B	−22.07	P, TWI, CE	A	<9.18	<0.37
NGC 1044	−21.48	P, TWI, CE	A	...	...
3C 75	−21.87	db, TWI	A	<9.28	<0.87
4C 1317B	−20.86	P	A	...	...
3C 78	−22.49	NP	E	<9.45	<0.28
NGC 1265	−22.95	P	A	<9.24	<0.27
3C 84	−22.76	D, J, TWI	E	10.72	0.90
0326+39	−20.42	P, CE	A	...	...
3C 111	−19.12	NP	E	10.29	>0.14
3C 120	−21.25	TWI, J	E	10.59	0.71
3C 129	−15.22	NP	A	...	...
0658+33	−22.49	M, TWI, CE	A	...	...
4C 3516A	−22.42	M, CE, TWI	A	...	...
4C 5316	−22.36	P, CE	A	...	...
0908+37	−22.95	(P, D)?	A	...	...
NGC 4789	−22.04	NP	A	...	...
3C 278	−20.35	db, TWI	A	<8.90	<0.34
NGC 4869	−19.91	TWI, J	A	...	...
4C 2947	−22.53	NP	A	...	...
NGC 5127	−20.18	NP	A	...	...
NGC 5490	−20.71	NP	A	...	...
3C 296	−22.74	P	A	<9.33	<0.38
3C 303	−21.89	NP	E	<10.90	<0.75
3C 305	−22.48	J, TWI	E	10.10	(0.66)
1450+28	−22.40	db, TWI	A	...	...
A2172		P, CE, TWI	A	...	...
4C 5337	−22.09	J	A	...	...
3C 371	−21.94	NP	E	10.23	0.44
3C 388	−22.94	M, CE, TWI	E	<9.88	<0.30
4C 4751	−23.04	J	A	...	...
3C 402N	−21.37	P, TWI	A	9.57	(0.24)
3C 405	−21.05	D, TWI	E	11.37	1.58
NGC 7052	−20.38	B	A	9.55	(0.46)
3C 433	−22.33	db	E	10.91	>0.25
3C 445	−21.19	NP	E	10.36	>0.62
3C 449	−21.28	P, CE, TWI	A	8.96	>0.17
2236+35	−20.48	NP	A	<8.98	<0.32
OZ 127		TWI	A	...	...
NGC 7626	−20.51	NP	A	...	...
3C 465	−20.00	P, CE, TWI	E	9.50	>0.49
4C 4763	−21.75	NP	A	...	...

[a] KEY TO ABBREVIATIONS.—B: boxy isophotes; CE: common envelope; D: central dust lane; db: dumbbell galaxy; J: jets or filaments; M: multiple companions; NP: no clear morphological peculiarities; P: companion galaxy located at projected distances shorter than 30 kpc; TWI: twisted isophotes.

where N is the total number of companion galaxies inside a radius r (in kpc); D_i, D_R are the measured diameters of the companion galaxy i and the radio galaxy, respectively, and d_{ir} is the projected distance between the companion galaxy i and the radio galaxy in kpc.

Therefore, P_n is related to the galaxy density within a certain radius, P_s to the relative size of the companion galaxies, P_d to the distance in units of 100 kpc and P_g to the gravitational potential of the companion galaxies if the relation $M \propto D^{1.5}$ (Dahari 1984) is assumed. Until a more detailed analysis is available (Pérez-Fournon and Colina 1990) using redshift information and elliptical isophote decomposition, one must consider these parameters as first-order approximation of the size, distance and interaction effect of the companion galaxies. The obtained results for a radius of 20 kpc are presented in Table 3.

TABLE 3
OPTICAL PARAMETRIZATION OF THE SAMPLE GALAXIES

Name	Abell Cluster	P_n	P_s	P_d	P_g
NGC 315	...	0	0	0	0
NGC 326	...	1	1.00	15.31	15.31
3C 31	...	1	0.33	10.13	1.92
NGC 541	A194	0	0	0	0
NGC 708	A262	2	0.98	11.03	4.00
NGC 708	COMP A	...	0.16	6.17	0.39
NGC 708	COMP B	...	0.82	4.86	3.61
0206+35	...	1	0.50	3.25	1.15
3C 66B	A347	1	0.20	10.25	0.92
NGC 1044	...	1	0.28	12.86	1.91
3C 75	A400	1	1.00	13.34	13.34
4C 1317B	A401	0	0	0	0
3C 78	...	0	0	0	0
NGC 1265	A426	1	0.26	4.96	0.68
3C 84	A426	0	0	0	0
0326+39	...	1	0.25	9.44	1.18
3C 111	...	0	0	0	0
3C 120	...	0	0	0	0
3C 129	...	0	0	0	0
0658+32	A567	1	1.00	8.67	8.67
4C 3156A	A568	1	0.68	4.58	2.57
4C 5316	...	0	0	0	0
0908+37	...	0	0	0	0
NGC 4789	...	0	0	0	0
3C 278	...	1	1.00	8.78	8.78
NGC 4869	A1656	0	0	0	0
4C 2947	...	0	0	0	0
NGC 5127	...	0	0	0	0
NGC 5490	...	0	0	0	0
3C 296	A1890	1	0.36	6.50	1.40
3C 303	...	0	0	0	0
3C 305	...	0	0	0	0
1450+28	A1984	1	1.00	4.18	4.18
A2172	A2172	1	0.40	5.94	1.50
4C 5337	A2220	0	0	0	0
3C 371	...	0	0	0	0
3C 388	...	1	0.15	8.07	0.47
4C 4751	...	0	0	0	0
3C 402N	...	1	0.33	5.54	1.05
3C 405	...	0	0	0	0
NGC 7052	...	0	0	0	0
3C 433	...	1	1.00	6.51	6.51
3C 445	...	0	0	0	0
3C 449	...	1	0.44	8.09	2.36
2236+35	...	0	0	0	0
OZ 127	A2572	1	0.33	7.61	1.44
NGC 7626	...	0	0	0	0
3C 465	A2634	1	0.30	14.85	2.44
4C 4763	...	0	0	0	0
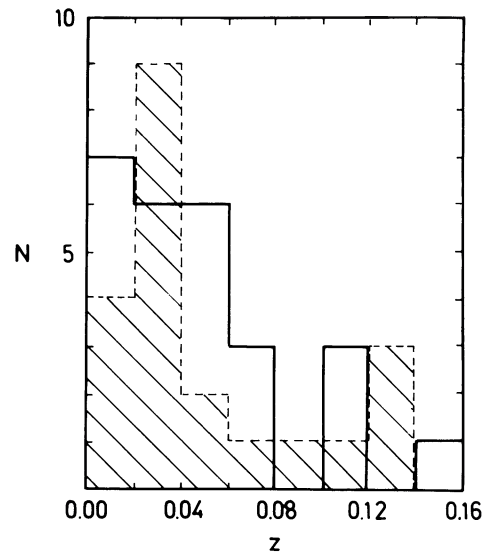
FIG. 1.—Histogram of the multicomponent (dashed and hatched trace) and isolated galaxies (solid trace) according to redshift.

Finally, although the redshift range is not large, it is important to ensure that the detection of companion galaxies is not redshift dependent. The histogram of the galaxy redshifts for galaxies for which there is no companion and for galaxies where one or more than one additional companion is detected within a radius of 20 kpc is presented in Figure 1. The redshift distribution of both samples is clearly similar, with median values of $z = 0.0334$ and $z = 0.0274$ for the galaxies with companions and isolated, respectively.

III. RESULTS

The first result of the present optical image survey is that a large number of these low-luminosity radio galaxies show a companion galaxy or have peculiar optical morphology not observed in isolated elliptical galaxies. It appears for this sample that as much as 50% show companion galaxies at projected distances shorter than 20 kpc and/or morphological peculiarities such as nonconcentric isophotes, twists, filaments, and asymmetric light distribution at surface brightness brighter than 24 mag arcsec^{-2} (see Table 2 and Paper I for details).

This result is very consistent with that of Heckman and collaborators (1986) based in a sample of very powerful radio galaxies. They concluded that at least 25%–30% of their galaxies with log $P_{408} \geq 25.5$ WHz^{-1} show strongly peculiar optical morphology that they consider as evidence of interaction/merging processes. In fact, 56% of their radio galaxies with redshift less than 0.15 were classified as peculiar in optical morphology. Also Hutchings (1987) found that in a sample of 50 high-luminosity radio galaxies and quasars in the redshift range 0.1–0.5, $\sim 80\%$ of the radio galaxies and 70% of the quasars were interacting with fainter companions.

A percentage as high as 13% of the sample (six galaxies) are dumbbell galaxies while the 32% of the galaxies (15) appear with a companion at distances shorter than 20 kpc, mean nucleus to nucleus separation of 12.8 kpc, and with a relative size 0.37 ± 0.18 (median value of 0.36) that of the radio galaxy. This size must be considered as an estimate since no detailed two-dimensional isophote analysis has been used to measure for instance the radius containing half of the light within each galaxy.

The total number of multicomponent galaxies (21) corresponds to a fraction of 45% of the galaxies in the sample. Before discussing further, we need to ask if this high fraction is due to projection effects or are in fact real physical companions. Schneider, Gunn, and Hoessel (1983) have studied a sample of brightest cluster galaxies located in Abell clusters. These authors observed that as many as 45% of the first ranked galaxies, regardless of the cluster richness, have a companion or companions at distances shorter than 16 kpc ($H_0 = 60$ km s^{-1} Mpc^{-1}) producing a multiple nucleus system. Since as much as 11 out of 21 of our multicomponents are located in Abell clusters, although not necessarily in the central regions, and some others in Zwicky clusters, we can estimate the fraction of these multicomponent systems which could be due to spurious projection effects. Following Schneider et al. (1983), the number of galaxies inside a certain radius r_s is obtained by the expression:

$$n_s = 1.44 N_c \ln \left[1 + (r_s/r_c)^2 \right] .$$

If in this expression we consider a typical core radius of the cluster of 300 kpc and a typical number of galaxies within this radius of $N_c = 20$, one obtains $n_s = 0.13$ galaxies within a radius of 20 kpc. Therefore, we expect that only a small fraction of our multicomponent galaxies, upper limit 13% (two to three), could be due to projection effects. This value is obviously the same as the total number of pairs of galaxies with separation distances shorter or equal to 20 kpc obtained using autocorrelation analysis (Dominguez-Tenreiro and Pozo-Sanz 1988). If one considers a $[1 + (r_s/r_c)^2]^{-1}$ law as the surface density profile and N_c and r_c as defined previously, we obtain 0.12 pair of galaxies.

Moreover, almost all of these galaxies, excluding some dumbbell galaxies or galaxies sharing common envelopes, show signs of distorted morphology such as nonconcentric isophotes indicating a real physical interaction (see Paper I; Lauer 1988). Therefore, at least 35% of the observed galaxies with radio jets consist of galaxies interacting with their nearby companions. This result is also obtained in an independent and complete sample of low-luminosity B2 galaxies with radio jets (Gonzalez-Serrano 1989).

The largest part of the sample, 55%, or 26 galaxies, consists of objects without companions at distances shorter than 20 kpc.

Considering the importance of interstellar/intergalactic material in the radio jet phenomenon and the expected gas fuel supply to the nuclear engine over large periods of time due to tidal interactions between disk galaxies (Lin, Pringle, and Rees 1988), one could ask how the presence of a companion galaxy at short distances, i.e., ongoing strong interaction, orbital motions, or merging, could enhance or produce a radio emission different from that of the more isolated galaxies where gravitational effects with more separated companions are nonexistent or less effective or where we see final stages of an interaction/merging process. Therefore, the observed sample has been divided into two subgroups that consider the existence or nonexistence of companion galaxies at distances shorter than 20 kpc. This division produces two samples with a similar number of objects: 21 and 26 for the multicomponent (dumbbell galaxies included) and isolated galaxies, respectively.

This subdivision is not an arbitrary one. There are many reasons suggesting that the presence of companions at distances shorter than 20 kpc have physical consequences. First, if
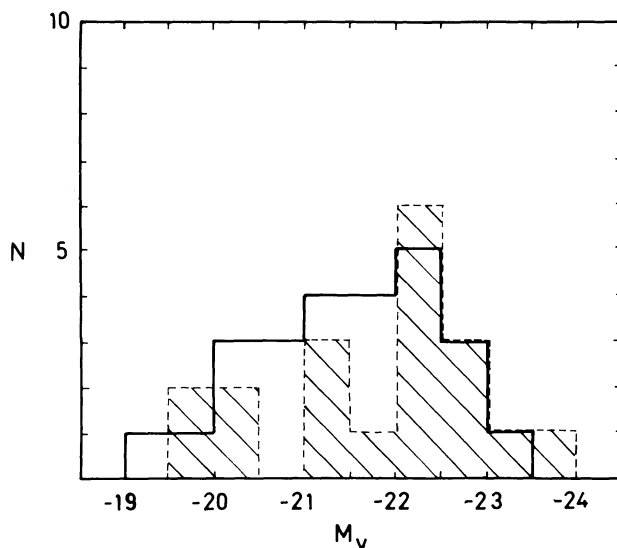
FIG. 2.—Same as in Fig. 1 but according to absolute visual magnitude. See § IIIa for details.

tidal forces are one of the mechanisms triggering the activity in galaxies, since $F_t \propto d^{-3}$, where d is the distance between the active galaxy and the companion, the shorter the interacting distance is, the stronger the tidal effect will be; second, Stoke (1978), concluding that the closer two galaxies are in projection, the greater the percentage of radio sources is, found a clear increase of the detection percentage at the separation index (angular separation of the pair on the sky divided by the mean angular diameter of the pair galaxies) decreases; third, Byrd et al. (1986) showed that a distance of closest approach of 10–20 kpc is adequate to obtain a substantial disturbance down to a radii of 1–2 kpc (center of the active galaxy) within the lifetime of the encounter; fourth, the presence of multiple nucleus first-ranked cluster galaxies (Hoessel 1980; Schneider et al. 1983) has been considered as a direct indication of galaxy cannibalism processes taking place.

a) Optical Absolute Magnitude

The two samples share the same optical absolute luminosity distribution over a range of 4.5 magnitudes (Fig. 2). The only difference is a slight excess in the median value. The multicomponent sample is almost half a magnitude brighter than the isolated one, with median value $M_v = -22.07$ as compared to $M_v = -21.75$ for the isolated one. This difference, 0.32 mag between the median values of the two samples, can be understood in part as the luminosity contribution of the near companion galaxy. In fact, if one considers the mean diameter (D) of the companion galaxy, dumbbell included, equal to 0.53 times that of the radio galaxy and one assumes M/L constant and the empirical relation $M \propto D^{1.5}$ (Dahari 1984), we get an excess of 0.35 mag with respect to the magnitude of the radio galaxy alone.

Therefore, if any systematic difference appears between these two samples, this cannot be associated to a different optical luminosity class but rather to a different parent galaxy or/and environment.

b) Optical Parent Galaxy

The two subsamples, multicomponent and isolated, respectively, can be characterized using the morphological param-
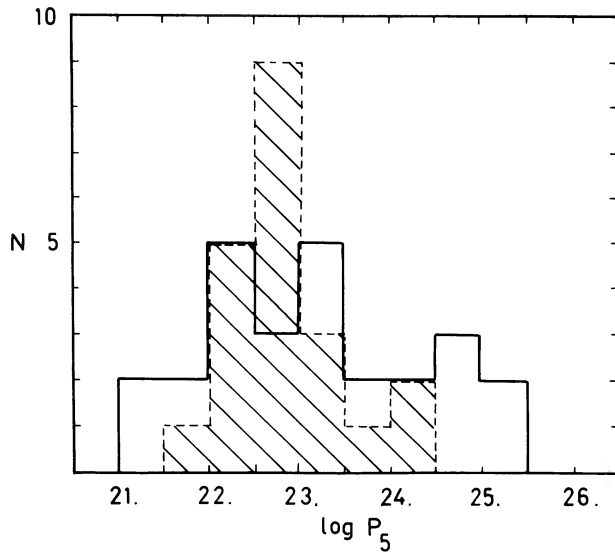
Fig. 3.—Same as in Fig. 1 but according to core radio luminosity at 5 GHz. See § IIIc for details.
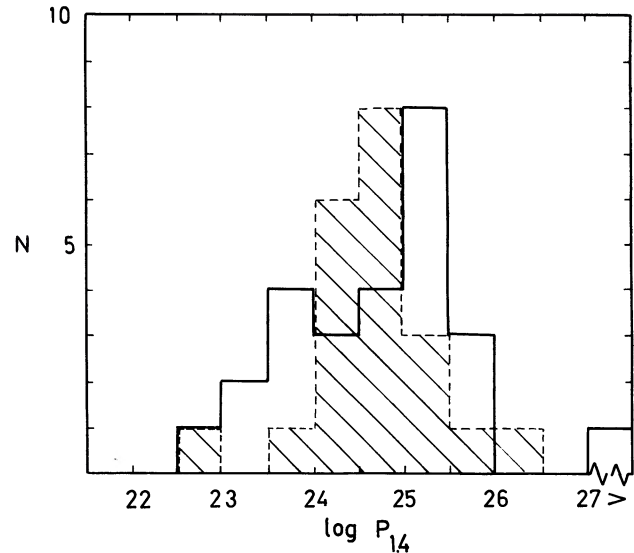
Fig. 4.—Same as in Fig. 1 but according to total radio luminosity at 1.4 GHz. See § IIIc for details.

eters defined in the previous section (§ IIc and Table 3). Accordingly, the multicompoennt sample will be characterized by median values $P_n = 1$, $P_s = 0.36$, $P_d = 8.09$, and $P_g = 2.36$. This sample can also be divided into two subsamples: (a) the dumbbell galaxies formed by two well-defined elliptical galaxies of the same size, i.e., similar mass, and separated by a mean projected distance of 10.5 kpc and (b) the multicomponent galaxies with a smaller nearby elliptical companion, relative size 0.37 ± 0.18 to that of the radio galaxy and mean separation between the nuclei of 12.8 kpc. If the mass-diameter $M \propto D^{1.5}$ relation is considered, we estimate the mass of the companion galaxy (M_c) within the range $0.06M_r \leq M_c \leq 0.37M_r$, with a mean value of 0.25 M_r, where M_r is the mass of the radio galaxy.

On the other hand, the isolated sample will be characterized by $P_n = P_s = P_d = P_g = 0$ within a radius of 20 kpc from the radio galaxy nucleus. Although some of the galaxies in this sample show filaments, tails, or jets (3C 84, 3C 120, and 3C 305 as examples), or have a very compact nucleus (3C 303, 3C 371, 3C 445, and 3C 120 as examples), most of them can be considered to be elliptical galaxies.

c) Core and Extended Radio Luminosities

Both the core and extended radio luminosities (Figs 3 and 4) show the isolated sample to be more distributed. In fact, as

much as 67% of the multicomponent galaxies have a core power (at 5 GHz) between 22.0 and 23.0 WHz^{-1}, median log $P_5^{core} = 22.79$, while only 31% of the isolated galaxies fall into this range, median log $P_5^{core} = 23.33$. For the extended radio emission, one finds that 67% of the multicomponent, median log $P_{1.4}^{total} = 24.68$, and 27% of the isolated galaxies, median log $P_{1.4}^{total} = 24.95$, have radio powers (at 1.4 GHz) in the 24.0–25.0 WHz^{-1} range. Also, isolated galaxies are, in median, brighter than multicomponent at 5 GHz and also at 1.4 GHz (see Table 4 for median values).

d) Core-extended Radio Luminosity Ratio

The multicomponent galaxies show up as an homogeneous sample, with 71% of the galaxies with $P_5^{core}/P_{1.4}^{total} \leq 0.03$ (median value $P_5^{core}/P_{1.4}^{total} = 0.0110$). On the other hand, the isolated sample, median $P_5^{core}/P_{1.4}^{total} = 0.0212$, has two distinct subsamples; 58% have $P_5^{core}/P_{1.4}^{total} \leq 0.03$ while the rest have $P_5^{core}/P_{1.4}^{total} \geq 0.06$ (Fig. 5).

e) Radio Jet Size

Concerning the radio jet size distribution (see Fig. 6), the multicomponent sample, median $d_{jet} = 25.3$ kpc, appears again as rather a homogeneous sample—67% of the galaxies with $10 \leq d_{jet} \leq 40$ kpc and not one with $d_{jet} \geq 80$ kpc. On the other hand, the isolated sample, median $d_{jet} = 29.3$ kpc, build

TABLE 4

MEDIAN VALUES OF THE PARAMETERS FOR DIFFERENT SAMPLES

Parameter	Isolated	3C Isolated	Multicomponent	3C Multicomponent
M_v	−21.75	−21.62	−22.07	−21.97
log P_5^{core}	23.33	24.55	22.79	22.77
log $P_{1.4}^{total}$	24.95	25.19	24.68	24.75
$P_5^{core}/P_{1.4}^{total}$	0.0212	0.0681	0.0110	0.0093
d_{jet}	29.3	23.2	25.3	28.7
P_n	0	0	1	1
P_s	0	0	0.36	0.35
P_d	0	0	8.09	8.44
P_g	0	0	2.36	2.14
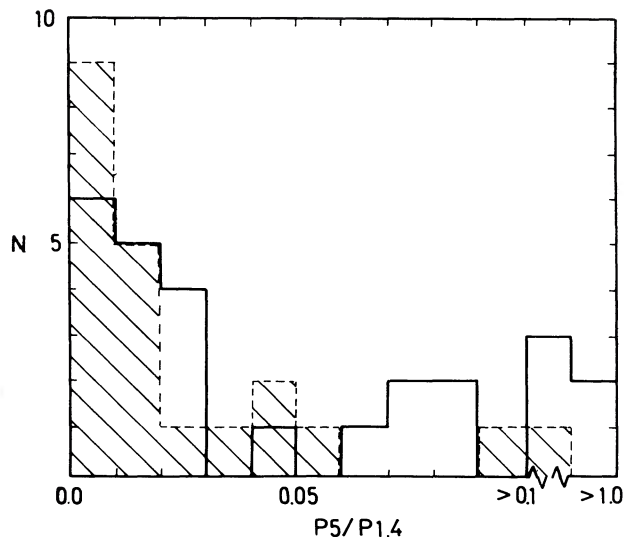
FIG. 5.—Same as in Fig. 1 but according to core/total radio luminosity ratio. See § IIId for details.

FIG. 6.—Same as in Fig. 1 but according to jet size. See § IIIe for details.

either very small jets, 50% with $d \leq 20$ kpc, or large jets, 23% with $d_{jet} \geq 80$ kpc.

f) Infrared Luminosities and Optical Emission Lines

Searching for intrinsic differences at infrared and optical wavelengths between our two subsamples, multicomponent and isolated, we look into the recent compilation of Golombek, Miley, and Neugebauer (1988). Both 60 and 100 μm luminosity data from the IRAS satellite as well as indication of optical emission lines appear in this compilation for 12 and 13 of our multicomponent and isolated galaxies. These data have been included in Table 2. The information on the spectral characteristics has been completed using mainly the Burbidge and Crowne (1979) catalog of radio galaxies. The spectra were classified as absorption (A in Table 2) when no indications of any emission line were present. On the contrary, when at least one luminous emission line is present, were classified as emission (E in Table 2).

Although the IRAS data are not complete for our sample, it seems that many of our isolated galaxies are more luminous in the far infrared (at 60 μm) than the multicomponent galaxies. In fact, eight out of 13 of these isolated galaxies (3C 84, 3C 11, 3C 120, 3C 303, 3C 371, 3C 405, and 3C 445) have luminosities well above $10^{10} L_\odot$; i.e., they are considered as powerful infrared sources. On the contrary only one out of 12 multicomponent galaxies (3C 433) has a luminosity above the previous limit. 3C 433 is a rather peculiar galaxy both at radio (van Breugel et al. 1983) and optical frequencies (Colina and Pérez-Fournon 1990).

Concerning the ratio $R[F(60~\mu m)/F(100~\mu m)]$, the previous isolated galaxies also show a larger R value than the multicomponent galaxies. Seven out of 13 isolated galaxies have $R \geq 0.5$, while only one multiple component galaxy (3C 75) appears with a R value larger than 0.5.

All these galaxies with large IRAS infrared luminosities have also indications of large amounts of ionized gas through the presence of emission lines in their spectra. Nine isolated galaxies show strong optical emission lines, while only two multicomponent galaxies have luminous lines in emission.
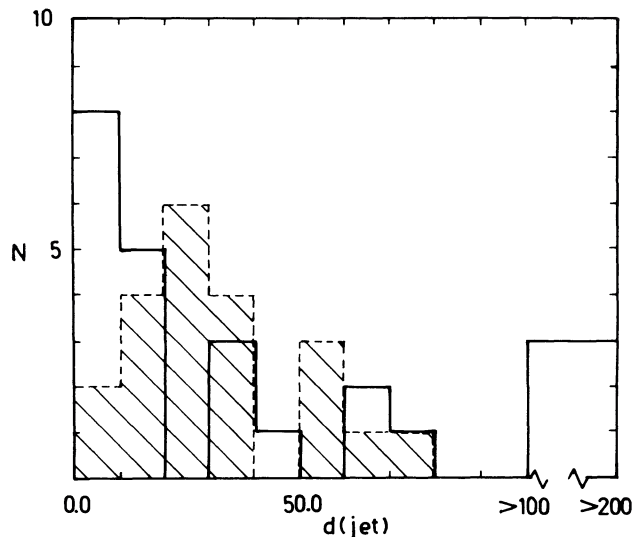
All the previous infrared and optical characteristics evidence the presence of large amounts of gas/dust and of a powerful ionizing source in a large fraction of our isolated galaxies. Since there is a correlation between radio luminosity and both optical and infrared luminosities (Golombek et al. 1988; Baum and Heckman 1989b), we expect that these galaxies will be the more luminous radio sources among the isolated sample. This is clearly the case since the median value of the core radio luminosity, log $P_5 = 24.19$ WHz^{-1}, is almost an order of magnitude larger than the median of the whole isolated sample (see Table 4).

IV. DISCUSSION

The results presented in the previous section have showed intrinsic differences in morphology as well as in optical, infrared, and radio properties between the multicomponent and the isolated galaxies in the present sample. How can one understand these differences? Are they due to a different parent galaxy population or to a different physical mechanism involved in the energy generation?

Heckman et al. (1986) have suggested, based in a sample of high-luminosity radio galaxies, that interaction or merging of disk galaxies is a characteristic process in these type of galaxies. Detailed models of disk-disk interactions (Toomre and Toomre 1972) indicate the formation of tails and bridges between interacting galaxies as a consequence of the tidal forces. Although interactions seem to play a crucial role in generating the activity of galaxies (Kennicutt and Keel 1984; Dahari 1984; Heckman et al. 1984, 1985; Byrd et al. 1986), a basic distinction exists between our nearby galaxies containing a radio jet and samples of Seyfert galaxies (Dahari 1984) or multiple nucleus active galaxies (Kollatschny and Fricke 1987): almost no indications of tails or filaments appear in our sample. However, many of our multicomponent galaxies present distorted and/or nonconcentric isophotes. Lauer (1988) found that, contrary to isolated ellipticals, nonconcentric isophotes are very common among multicomponent elliptical galaxies. This feature presents the strongest evidence of components in tidal interaction. This is understood to be a consequence of the ratio between the orbital/crossing time scale of the stars at a certain radius $[T_{orb}(r)]$ and the interaction

time scale between the radio source and the near companion galaxy (T_{int}). If this ratio, $T_{orb}(r)/T_{int}$, is of the order of one or less, the stars within this radius will be affected by a strong gravitational perturbation over a large fraction of its orbital time and consequently nonconcentric isophotes will be developed against the external envelopes.

Therefore, if interaction is one of the main mechanisms triggering the activity in galaxies, one can suggest that interaction/merging between different parent galaxies will manifest different kinds of activity. Interaction between gas-rich galaxies could produce Seyfert activity (see previous references) while between gas-poor elliptical galaxies (our multicomponent sample) could only generate radio activity. The same process between spheroidal-disk galaxies (our isolated sample?) will produce a type of activity in between the two previous extreme cases.

In the following, based in the results presented in section three, we will look in more detail to the above-mentioned hypothesis.

a) Isolated sample: Systems Involving Gas-rich Disk Galaxies

The results presented in § III indicate that what we call an isolated sample is very heterogeneous, showing no particular trend in properties. However, it seems that an important fraction of the sample shows properties of gas-rich systems that could originate as interactions/mergers involving at least one disk galaxy. This idea was suggested by Heckman and collaborators (Heckman et al. 1986) based in the results of a sample of high luminosity radio galaxies.

In fact, one of our isolated galaxies (3C 305) has been considered (Heckman et al. 1982) as the merger product of a luminous early-type galaxy and a late-type, gas-rich galaxy. Its general properties—presence of strong optical emission lines, large 60 μm luminosity, warm luminous IRAS source [i.e., large $F(60 \mu m)/F(100 \mu m)$ ratio], and small-size radio jet—are very similar to those observed in many other of the isolated galaxies. Also, Hu and collaborators (1983) suggested that the 3C 84 system of filaments is due to the collision between a late-type spiral galaxy and the accretion flow of the central galaxy in the Perseus cluster.

The presence of emission lines are evidence of the existence of large amounts of ionized gas and of a powerful ionizing source, while the infrared properties are most likely due to warm dust emission heated by recently formed massive stars (Telesco, Wolstencroft, and Done 1988) or by the central nonthermal source (Golombek et al. 1988). The 60 μm mean luminosity of our isolated sample for which IRAS fluxes have been measured (see Table 3) is similar, although with a larger dispersion, to that obtained for a sample of Markarian starburst galaxies [$L(60 \mu m) = 10.16 L_{\odot}$; Deutsch and Willner 1986], while it is a factor of 5 smaller than in IRAS Seyfert galaxies (IRAS Circ. No. 11, 1984; de Grijp et al. 1985). Also, many of these luminous IRAS sources (seven out of 13) have $F(60 \mu m)/F(100 \mu m)$ larger than 0.5. This value is considered as characteristic of warm dust reradiation in Arp-Madore interacting galaxies (Telesco et al. 1988). The same conclusion was reached by Young et al. (1986); they found $F(60 \mu m)/F(100 \mu m)$ equal to 0.71 and 0.38 for a sample of interacting/merging and isolated galaxies, respectively.

Also, the radio jet size with 50% of the sample presenting $d(\text{jet}) \leq 20$ kpc, i.e., well inside the main body of the optical parent galaxy, is reminiscent of the elongated radio morphologies detected in Seyfert galaxies (Wilson 1983). The radio jet

could be disrupted if the interstellar medium of the galaxy is rich in cold gas sharing the rotational motion of the galaxy or having a chaotic velocity behavior.

Although all these characteristics are consistent and support the idea that a large fraction of our isolated sample is formed by gas-rich galaxies or by the interaction/merging product of elliptical-disk galaxies, this may well not be the whole history. Some of the strong IRAS sources—3C 303, 3C 371, or 3C 445—show an elliptical morphology but with a very compact optical nucleus. These systems could be classified as N galaxies. Furthermore, superluminal motions have been measured in 3C 120 (Walker et al. 1987), indicating that physical phenomena such as beamed relativistic jets could also be present. Finally, the largest fraction of the isolated sample is formed by galaxies which can be classified as ellipticals with no clear signs of any morphological peculiarity and showing distinctive radio properties (see § IVc).

b) Multicomponent Sample: Systems Involving Gas-poor Ellipticals?

The multicomponent sample can be divided in two subgroups: galaxies with a dumbbell structure, i.e., systems formed by two almost equal massive ellipticals, or those with a large nearby companion.

Concerning galaxies with dumbbell morphology, we can consider two cases as standard ones. The first one is the system formed by NGC 4782 and NGC 4783, which shows clear indications of ongoing physical interaction in the form of twisted, nonconcentric isophotes and common envelope (Paper I). This galaxy has been modeled in detail by Borne and coworkers (Borne et al. 1988) as a high-speed encounter ($\langle V/\sigma \rangle = 1.95$) of two almost equal massive galaxies (mass ratio 0.7) which are at 8×10^6 yr after pericenter passage and which will merge within 8×10^8 yr. The second one is 3C 75, which appears as a projected pair of equal ellipticals with a slightly asymmetrical outer envelope (Paper I). It shows nonconcentric isophotes in the northern galaxy if a detailed two dimensional isophotal fitting is used (Lauer 1988). Also, according to Lauer (1988), the southern galaxy has a powerful luminosity profile while the northern galaxy follows a de Vaucouleur law. At optical wavelengths there is no other clear evidence of physical interaction while at radio frequencies, the complex system of radio jets generated in both galaxies favor the hypothesis of an interaction.

B2 0206 + 35 and 3C 465 can be considered as good representative examples of multicomponent galaxies with a large nearby elliptical companion. B2 0206 + 35 shows an isophote twist of 60° toward the position angle joining the nuclei of the two galaxies (see Paper I). Gonzalez-Serrano (1989) measured nonconcentric isophotes in both the main radio galaxy and the smaller companion going up to $\Delta R/R = 0.2$–0.3 for the companion where R indicates the radius. Also Valentijn and Casertano (1988) have measured a relative velocity of 70 km s^{-1} between the radio galaxy and its companion. These features can be interpreted as a recent and ongoing low-velocity encounter.

Similar results are observed by Lauer (1988) for 3C 465. The nucleus of the radio galaxy is displaced from its envelope up to a value of $\Delta R/R = 0.1$ in the direction toward the secondary. The smaller companion presents, on the other hand, a twist of the isophotes toward 3C 465 as well as a truncation of the luminosity profile. In this case the measured relative velocity

(Valentijn and Casertano 1988) is 997 km^{-1}. This could be considered as a fast, interpenetrating encounter.

The lack of strong optical emission lines (on 3C 388 and 3C 433 show luminous emission lines) and strong powerful infrared emitters [only 3C 433 has $L(60\ \mu m) \geq 10^{10}\ L_\odot$] in these galaxies indicate the lack of large amount of gas/dust and nonthermal UV ionizing continuum in these systems.

On the other hand, the morphology of the radio emission support the idea of gas-poor spheroidal systems in interaction. Shaver *et al.* (1982) showed from a completed sample of radio sources that both the C and S distortions (mirror and inversion symmetry) only occur when other galaxies are located near the radio source. These morphologies are interpreted (Wirth *et al.* 1982) as consequence of orbital circular motions, mirror symmetry with wiggles, or tidal interaction during the close passage of an unbound system producing precessional effects, i.e., inversion symmetry. In fact, many of our multicomponent galaxies, NGC 326, 3C 31, NGC 708, NGC 1044, 3C 449, or 4C 35.03, show any of these morphologies while other dumbbell galaxies like 3C 75 (Owen *et al.* 1985) or 3C 433 (van Breugel *et al.* 1984) show a more complex morphology.

Also, the tendency of an alignment between the double-sided radio jet axis and the direction joining the two galaxy nuclei although not yet clearly understood, could be somehow related to the presence of a large companion with mean size one-fourth that of the radio source, at very short distances, typically less than 20 kpc.

c) Radio Emission versus Interaction and Parent Galaxy

We have shown previously that our multicomponent galaxies have very homogeneous set of radio properties while the isolated galaxies are more heterogeneous. Also, a large fraction of our isolated galaxies show strong indications of large amounts of gas/dust and powerful ionizing source through the presence of large emission lines and *IRAS* luminosities.

Performing the χ^2 test for the two samples, isolated and multicomponent, with respect to the different parameters characterizing the radio emission, we obtain that the isolated sample shows a larger core radio luminosity (log P_5^{core}) and smaller jet size (d_{jet}) than the multicomponent sample at better than 90% and 95% confidence level, respectively. In the case of the other two parameters (log $P_{1.4}^{total}$, $P_5^{core}/P_{1.4}^{total}$) the differences are statistically less significant.

Although the performed statistical tests do not indicate any big difference with a large confidence level between the two samples, we believe that this can be due to two effects. One is the small number of galaxies in each sample. This makes it very difficult to get any significant conclusion unless the distributions in the parameter space are radically different. The second effect is that, as already discussed, we are mixing in the isolated sample two types of host galaxies, gas-poor ellipticals, and gas-rich systems, and this could smooth any difference.

If we remove from both samples, multicomponent and isolated, the galaxies which can be considered as gas-rich systems—i.e., those showing emission lines in their spectra—we could see the relative importance of interactions and type of host galaxy in generating different kinds of radio galaxies. We have now three different samples: the isolated ellipticals (17), the multicomponent ellipticals (17) and the gas-rich galaxies (13). The distribution of these samples according to their radio properties are presented in Figures 7–10.

The larger differences between the three samples appear when the radio luminosities are considered. The multicomponent ellipticals are still building very homogeneous low-luminosity radio sources with 82% of the sample having log
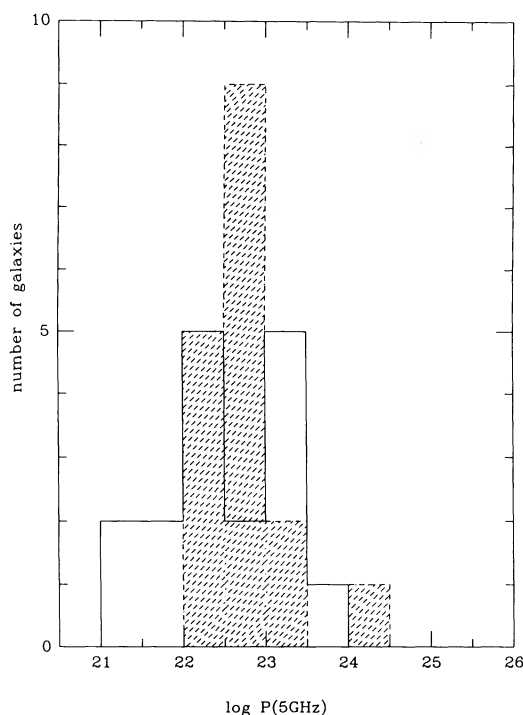
FIG 7a
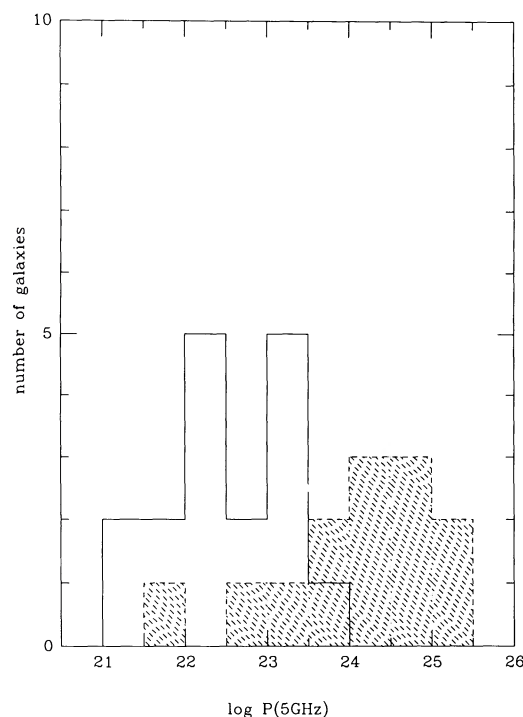
FIG. 7b

FIG. 7.—(a) Histogram of the isolated ellipticals (*solid trace*) and gas-rich systems (*dashed and hatched trace*) according to core radio luminosity at 5 GHz. (b) Same as previous figure but for isolated ellipticals (*solid trace*) and multicomponent ellipticals (*dashed and hatched trace*). See § IVc for discussion.
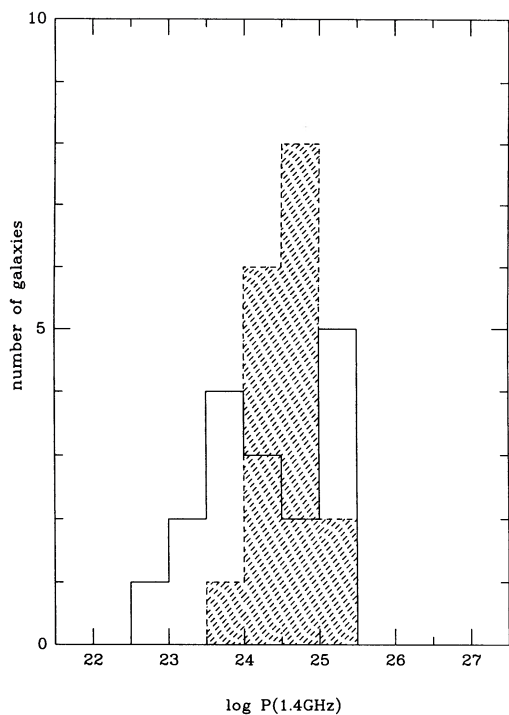
FIG. 8*a*
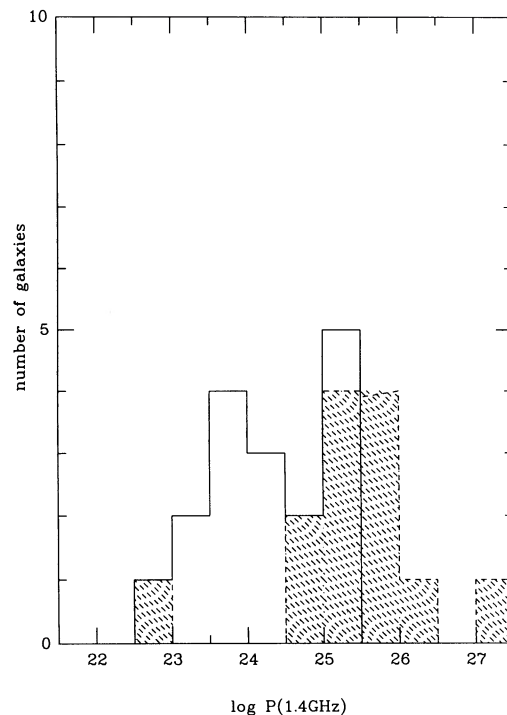
FIG. 8*b*

FIG. 8.—(*a*) and (*b*) Same histogram as in Figs. 7*a* and 7*b* but according to total radio luminosity at 1.4 GHz. See § IV*c* for discussion.

P_5^{core} between 22.0 and 23.0 WHz^{-1} and log $P_{1.4}^{total}$ between 24.0 and 25.0 WHz^{-1}. The isolated elliptical galaxies also produce low-luminosity radio sources spread over a range of almost three orders of magnitude in radio luminosity. The gas-rich galaxies are the most powerful radio sources in our sample. They are almost 100 times brighter than any of the other two

samples. This result is statistically significant at better than 90% confidence level.

Concerning the other two parameters, the differences are less clear. However, none of the multicomponent ellipticals produce a very large jet, size larger than 100 kpc, while the other two samples are capable of generating such a jet. This

FIG. 9*a*
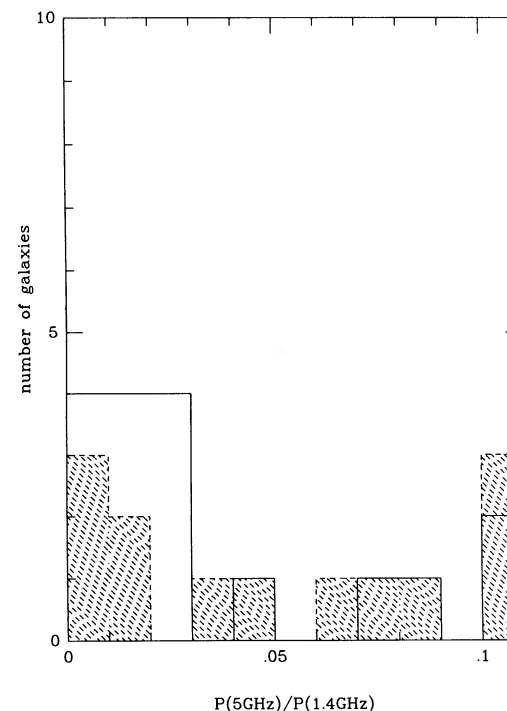
FIG. 9*b*

FIG. 9.—(*a*) and (*b*) Same histogram as in Figs. 7*a* and 7*b* but according to core/total radio luminosity ratio. See § IV*c* for discussion.
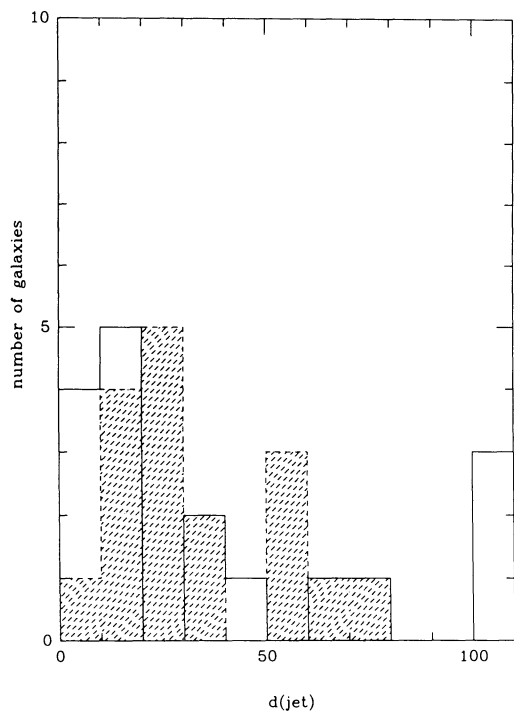
FIG. 10a
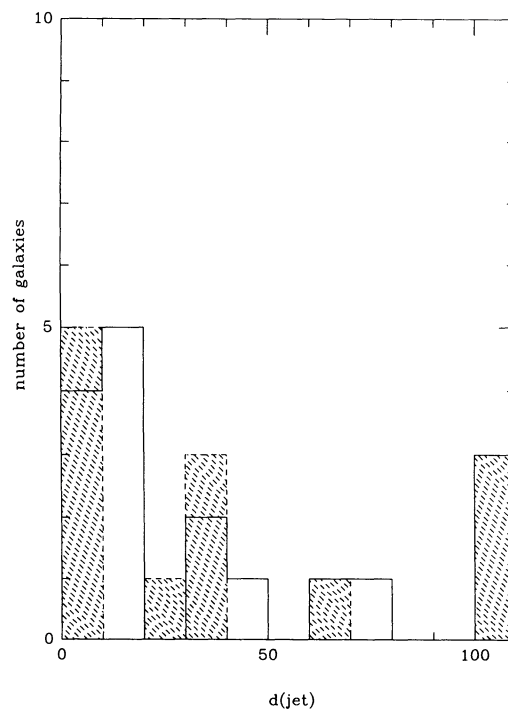
FIG. 10b

FIG. 10.—(a) and (b) Same histogram as in Figs. 7a and 7b but according to jet size. See § IVc for discussion.

can be understood as a combination of more scarce environments and/or more energetic radio sources. In these cases will be more difficult to stop or disrupt the radio jet. Also the gas-rich galaxies show a uniform distribution in $P_5^{core}/P_{1.4}^{total}$ indicating that the core and total radio luminosities are not well correlated.

Looking at these results it seems that the presence of gas, i.e., amount of gas, independent of its origin, available for fueling in the central parts of the galaxies, is more important than strong interaction processes, at least between ellipticals, in generating powerful radio luminosity sources. However, the ongoing interaction process between ellipticals seems to control the energy generation, possibly through the way the gas/stars fell into the nucleus, producing a very well defined type of radio sources concerning their luminosity and the size and morphology of the jet.

Finally, what we call isolated ellipticals could be affected by interactions with companions at much larger distances or affected somehow by a different environment producing a more heterogeneous range of low-luminosity radio sources.

The central parts of a small galaxy can survive the merging process with a more massive galaxy and be located as a merger residual in the nucleus of the larger galaxy (Balcells and Quinn 1989). Therefore, intrinsic differences in the central parts of the galaxies like compact optical cores within ellipticals (3C 303, 3C 371, or 3C 445), disk substructures or dust lanes (3C 31, Cyg A, NGC 708) could teach us something about the past interaction/merging history of the radio source, and therefore we could learn more about how interactions/merging, activity, and parent host galaxy are connected. High spatial resolution observations with the Hubble space telescope would greatly improve our understanding of the physical phenomena present in the nucleus of these galaxies.

V. CONCLUSIONS

This paper has presented the first systematic survey at optical wavelengths of galaxies with detected radio jets using CCD imaging. The main conclusions can be summarized as follows:

1. Around 50% of the low-redshift ($z \leq 0.15$) galaxies with radio jets have a large nearby companion and/or show peculiar optical morphology not detected in isolated ellipticals. This agrees with the results obtained for high luminosity radio galaxies and quasars (Heckman et al. 1986; Hutchings 1987).

2. Forty-five percent of the objects in this sample have a companion galaxy at distance shorter than 20 kpc. Of these, 13% are dumbbell galaxies, and 32% have a large companion with a relative mean size 0.37 that of the radio galaxy and at a mean distance of 12.8 kpc. Taking into account the projection effects, we conclude that at least 35% of the radio jet galaxies are multicomponent galaxies in physical interaction.

3. The radio jet sample has been divided into two subsamples: the multicomponent sample formed by these galaxies with a companion at distances shorter than 20 kpc, i.e., strong tidal effects due to ongoing physical interaction/merging processes, and the isolated sample formed by these galaxies with no companions at distances shorter than 20 kpc, i.e., much weaker tidal effects with far away galaxies or galaxies which are merger products.

4. The multicomponent galaxies, form a very homogeneous sample with the following properties: 67% have $22.0 \leq \log P_5^{core} \leq 23.0$ WHz^{-1}, 67% have $24.0 \leq \log P_{1.4}^{total} \leq 25.0$ WHz^{-1}, 67% have $10.0 \leq d$(jet) ≤ 40.0 kpc, 71% have $0.00 \leq P_5^{core}/P_{1.4}^{total} \leq 0.03$, while they do not present indications of large amounts of gas and dust, i.e., lack of strong optical emission lines and powerful infrared emission. The isolated sample has more heterogeneous radio properties while the presence of

emission lines and 60 μm luminosity in excess of 10^{10} $L_\odot$ indicates large amounts of gas and warm dust in a large fraction of these galaxies.

5. The intrinsic differences detected in optical morphology, radio jet structure, infrared, and radio properties between the multicomponent and isolated samples are explained in terms of a different parent galaxy and interaction processes. The more powerful radio sources appear in gas-rich galaxies. Galaxies in interaction with a large elliptical companion build lower luminosity radio sources with very homogeneous radio properties. Isolated ellipticals also build low-luminosity radio sources but more heterogeneous than the multicomponent galaxies.

6. We conclude that, at least among galaxies with radio jets, the amount of gas available and the interactions could control the energy generation, producing a very well defined type of radio source. Some other parameters, such as intrinsic differences in the structure of the central parts of the radio galaxy, can also be important and must be investigated in more detail.

The results presented here give a first qualitative picture of a possible scenario to explain different kinds of radio sources. A more detailed work in progress, involving two-dimensional modeling of the stellar isophotes together with spectroscopic studies, will permit us to quantify parameters like presence of disk structures or peculiar stellar velocity dispersions in the nucleus, relative velocities of the companions, amount of cold and hot gas, and type of interaction and relate these with the radio source parameters in order to understand this phenomenon more deeply. New observations of more radio jet galaxies would also help to check the previous ideas.

REFERENCES

Balcells, M., and Quinn, P. 1989, preprint.
Baum, S. A., and Heckman, T. 1989a, *Ap. J.*, **336**, 681.
———. 1989b, *Ap. J.*, **336**, 702.
Baum, S. A., Heckman, T., Bridle, A., van Breugel, W., and Miley, G. 1988, *Ap. J. Suppl.*, **68**, 643.
Begelman, M. C., Blandford, R. D., and Rees, M. J. 1980, *Nature*, **287**, 307.
Borne, K., Balcells, M., and Hoessel, J. G. 1988, *Ap. J.*, **333**, 567.
Bridle, A. H. 1984, *A.J.*, **89**, 979.
Bridle, A. H., and Perley, R. A. 1984, *Ann. Rev. Astr. Ap.*, **22**, 319.
Burbidge, G., and Crowne, A. H. 1979, *Ap. J. Suppl.*, **40**, 583.
Byrd, G. G., Valtonen, M., Sundelius, B., and Valtaja, L. 1986, *Astr. Ap.*, **166**, 75.
Colina, L., and Pérez-Fournon, L. 1989, *Ap. J. Suppl.*, in press (Paper I).
———. 1990, in preparation.
Dahari, O. 1984, *A.J.*, **89**, 966.
de Grijp, M. H. K., Miley, G. K., Lub, J., and de Jong, T. 1985, *Nature*, **314**, 240.
Deutsch, L. K., and Willner, S. P. 1986, *Ap. J. (Letters)*, **306**, L11.
Dominguez-Tenreiro, R., and del Pozo-Sanz, R. 1988, *Ap. J.*, **324**, 677.
Fricke, K. J., and Kollatschny, W. 1987 in *IAU Symposium 121, Observational Evidence of Activity in Galaxies*. ed. Ye. E. Khachikian, K. J. Fricke, and J. Melnick, (Dordrecht: Reidel), p. 371.
Gonzalez-Serrano, J. I. 1989, Ph.D. thesis, La Laguna University.
Golombek, D., Miley, G. K., and Neugebauer, G. 1988, *A.J.*, **95**, 26.
Heckman, T. M., Bothun, G. D., Balick, B., and Smith, E. P. 1984, *A.J.*, **89**, 958.
Heckman, T. M., Carty, J. J., and Bothun, G. D. 1985, *Ap. J.*, **288**, 122.
Heckman, T. M., Smith, E. P., Baum, S. A., van Breugel, W. J. M., Miley, G. K., Illingworth, G. D., Bothun, G. D., and Balick, B. 1986, *Ap. J.*, **311**, 516.
Hoessel, J. G. 1980, *Ap. J.*, **241**, 493.
Hu, E. M., Cowie, L. L., Kaaret, P., Jenkins, E. B., York, D. G., and Roesler, F. L. 1983, *Ap. J. (Letters)*, **275**, L27.
Hutchings, J. B. 1987, *Ap. J.*, **320**, 122.

IRAS Circ., No. 11, 1984 (*Astr. Ap.*, **134**, C5).
Kennicutt, R., and Keel, W. 1984, *Ap. J. (Letters)*, **279**, L5.
Kollatschny, W., and Fricke, K. J. 1987 in *IAU Symposium 121, Observational Evidence of Activity in Galaxies*. ed. Ye. E. Khachikian, K. J. Fricke, and J. Melnick (Dordrecht: Reidel), p. 377.
Lauer, T. R. 1988, *Ap. J.*, **325**, 49.
Lilly, S. J., and Prestage, R. M. 1987, *M.N.R.A.S.*, **225**, 531.
Lin, D. N. C., Pringle, J. E., and Rees, M. J. 1988, *Ap. J.*, **328**, 103.
Owen, F. N., O'Dea, C. P., Inone, M., and Eilek, J. A. 1985, *Ap. J. (Letters)*, **294**, L85.
Pérez-Fournon, I., Colina, L., Gonzalez-Serrano, J. I., and Biermann, P. 1988, *Ap. J. (Letters)*, **329**, L81.
Pérez-Fournon, I., and Colina, L. 1990 in preparation.
Schneider, D. P., Gunn, J. E., and Hoessel, J. G. 1983, *Ap. J.*, **268**, 476.
Shaver, P. A., Danziger, I. J., Ekers, R. D., Fosbury, R. A. E., Goss, W. M., Malin, D., Moorwood, A. F. M., and Wall, J. V. 1982 in *IAU Symposium 97, Extragalactic Radio Sources*, ed. D. J. Heeschen and C. M. Wade (Dordrecht: Reidel), p. 55.
Stoke, J. 1978, *A.J.*, **83**, 348.
———. 1979, *Ap. J.*, **230**, 40.
Telesco, C. M., Wolstencroft, R. D., and Done, C. 1988, *Ap. J.*, **329**, 174.
Thuan, T. X., and Gunn, J. E. 1976, *Pub. A.S.P.*, **88**, 543.
Toomre, A., and Toomre, J. 1972, *Ap. J.*, **178**, 673.
Valentijn, E. A., and Casertano, S. 1988, *Astr. Ap.*, **206**, 27.
van Breugel, W., Balick, B., Heckman, T. M., Miley, G. K., and Helfand, D. 1983, *A.J.*, **88**, 40.
Vettolani, G., and Gregorini, L. 1988, *Astr. Ap.*, **189**, 39.
Walker, R. C., Benson, J. M., and Unwin, S. C. 1987, *Ap. J.*, **316**, 546.
Wilson, A. S. 1983, in *Highlights Astr.*, **6**, 467.
Wirth, A., Smarr, L., and Gallagher, J. S. 1982, *A.J.*, **87**, 602.
Young, J. S., Kenney, J. D., Tacconi, L., Claussen, M. J., Huang, Y. L., Tacconi-Garman, L., Xie, S., and Schloerb, F. P. 1986, *Ap. J. (Letters)*, **311**, L17.

LUIS COLINA: Space Telescope Science Institute, Homewood Campus, 3700 San Martin Drive, Baltimore, MA 21218

ISMAEL PÉREZ-FOURNON: Instituto de Astrofísica de Canarias, La Laguna, Tenerife, Spain